

Species Concentration Gradient Method for Solution of Reacting Flow

I. Ahmad*, R. Ahmad, S. Tahir, S. Ahmad

Department of Nuclear Engineering (DNE), Pakistan Institute of Engineering and Applied Sciences (PIEAS), Islamabad 45650, Pakistan.

ABSTRACT

In this article, a new error balance approach utilizing local error per unit step (LEPUS) control strategy has been developed. The error control strategy has been upgraded to incorporate the temporal and spatial discretization error by an adjusting parameter, which has been linked with species gradient present in the chemical mechanism. The accuracy and efficiency of the proposed improved LEPUS (ILEPUS) have been checked by solving the one-dimensional compressible gaseous flow in the absence of a reaction mechanism and compared with the old local error per step (LEPS) and traditional LEPUS strategies. With respect to the concentrations of nitrogen oxide and nitrogen dioxide for the winter season, the simulation predictions have been found to have a positive correlation with the recent experimental data collected in Changchun city, China. For further insights into the scheme, both one- and two-dimensional reacting flows with complex chemical reactions have also been solved using ILEPUS and LEPS, where the ILEPUS scheme has proven better performance as compared with LEPS and LEPUS.

Keywords: Atmospheric Chemistry Model, Error Balance Approach, Species Concentration Gradient, Chemical Mechanism, Nitrogen Oxides

1. Introduction

The burning of fossil fuels is generally an enriched source of nitrogen and sulfur oxides. As a result of increased use of fossil fuels, their releases have more than doubled in the last century. Consequently, an alarming level of global warming and the adverse effect of pollutants on the environment have motivated researchers to study them thoroughly in the context of their effect on the atmosphere. The main sources of these pollutants are emissions from power plants, motor vehicles, etc. which are enriched sources of Volatile Organic Compound (VOCs), CO, CO₂, Nitrogen Oxides (NO_x), Sulfur Oxides (SO_x) and particulate matter (PM) [17]. The photochemical reaction converts NO_x into ozone at a large distance downwind from the source. Similarly, other products such as CO and PM are known to have adverse health effects. In addition, the emitted pollutants from these sources include hundreds of species and therefore, achieving a high spatial resolution are challenging. Moreover, the governing equations that handle these models are characterized by coupling, non-linearity, and stiffness. These factors emphasized that a specialized solver with error control should be developed for dealing with such a complex model. The reason for the number of chemical rate equations, which needs to be solved, increases with the number of species; and for comprehensive analysis, three-dimensional calculations are required. Detailed analysis is also important because the limited capability of a comprehensive chemistry/transport model raised issues for environmental scientists and policymakers [2].

Historically, the development of the most advanced atmosphere and chemistry models goes back to the late 1970s and early 1980s. After that, these models have been updated continuously to develop efficient and well-structured solvers. So far, remarkable progress has been made to counter the stiffness problem by applying different pre-conditioner, parameter optimization and sophisticated error control strategy. The method of lines is preferred to avoid the splitting error for a stiff and coupled system of equations [3, 4]. Despite

the other factors, estimating and controlling the computational error has a vital role in the efficiency and accuracy of the stiff solvers.

For an efficient solution of the stiff partial differential equation, a rigorous error analysis should be performed in spatial and temporal discretization schemes. Error analysis techniques may be divided into two categories, local error per step (LEPS) and local error per unit step (LEPUS). Adequate literature is available on LEPS compared to the limited literature on LEPUS control strategy. It was introduced in the work presented in ref. [5] and further extended by other groups [3] and [6]. The method was used to solve the Euler equations and was also applied to study a combustion problem [7]. Extensive research has revealed that another contribution in the current field is the work of [8] as they have applied it to solve the Euler equations.

The LEPUS strategy establishes a link between global error and accuracy tolerance, which is not the case with the LEPS control strategy. Also, the latter strategy exploits the local truncation error and the solver performs better with the first strategy [5, 9]. The ILEPUS applies the error balance approach in the framework of LEPUS control strategy that is not present in the LEPS control strategy. This form of the error balance approach is generally not suitable for stiff problems discussed here due to the variation in spatial error at each time step. It takes much more time steps in the case of spatial error that normally happened at the end of the time at which the solution is sought. Initially, the spatial error is too high, and the solution is accepted even though the results have not been converged. Therefore, these two drawbacks have been controlled to improve typical LEPUS strategy in this study.

The prime aim of this study is to devise a robust and efficient scheme to solve only chemical reaction models. Therefore, ILEPUS was proposed as a new error balance approach because typical LEPUS was unable to provide an optimal performance of the stiff solver. The reason is the

*Corresponding author: idrees@pieas.edu.pk

provided tolerance, which varies according to the spatial error at each step. Spatial error is the difference between the primary and secondary solutions of the model equation that is obtained using various discretization schemes and source term integration method. The novel idea is introduced by varying the adjusting parameters adaptively and is linked to the difference in species gradient using the arc-length adaptive mechanism in time [9]. In ILEPUS both the step size acceptance and rejection procedure are modified that helped in improving the performance by reducing the time step and other statistical data. The NDF2 method is used as a time Integrator due to its less truncation error and better performance in atmospheric modeling compared with BDF2 method [1]. Moreover, the other optimization is performed by connecting the Jacobian matrix calculation at each grid point with a spatial discretization error at each time step.

In this paper, one-dimensional problems have been tackled with ILEPUS and LEPS schemes, and comparisons of results have shown an excellent agreement with the experimental data [10]. It was also noted that nitrogen oxide trends are also same everywhere and that the only difference is in concentration. Furthermore, a peak was observed around 9 AM and can be seen in [11-13]. The accuracy between the expected results and the simulated results is verified with the correlation coefficient indicated in [12]. In this article, the development of ILEPUS strategy with adaptive error control, numerical comparison to the atmospheric reaction-diffusion problem and correlation with experimental data were discussed.

2. Materials and Methods

2.1 Atmospheric diffusion equation

The transportation of pollutants in the air is usually modelled by the atmospheric diffusion equation and its 2D case is presented as follows [5].

$$\frac{\partial C_i}{\partial t} + \frac{\partial(uC_i)}{\partial x} + \frac{\partial(vC_i)}{\partial y} = \frac{\partial}{\partial x} \left(K_x \left(\frac{\partial C_i}{\partial x} \right) \right) + \frac{\partial}{\partial y} \left(K_y \left(\frac{\partial C_i}{\partial y} \right) \right) - (k_{1,i} + k_{2,i})C_i + E_i + R_i(C_1, C_2, \dots, C_N), \tag{1}$$

where, N , C_i , E_i and R_i are the number of species being modeled, concentration of the i^{th} pollutants, emission source of i^{th} species and chemical reaction of i^{th} species, respectively. Furthermore, u , v are the wind velocity along the coordinated axes, K_x , K_y are the diffusivity coefficients and $k_{1,i}$, $k_{2,i}$ are the dry and wet deposition coefficients of the i^{th} species.

2.2 Implementation details

Details of implementing an optimized form of the LEPLUS control strategy [3, 5, 8] are linked by writing Eq. (1) in the following compact form:

$$\frac{\partial u}{\partial t} + \alpha \frac{\partial u}{\partial x} = \psi(u) \tag{2}$$

Generalized procedure for this is to apply the method of lines that will reduce the system of ordinary differential equations as follows:

$$\dot{V} = F_N(t, V(t)) \tag{3}$$

with known initial condition $U(0)$ and $[V(t_n)]_{n=0}^p$ is numerical approximate solution at a set of discrete time points $0 = t_0 < t_1 < t_2 \dots t_p = t_f$ generated by time integrators. The key idea of this error control strategy is to estimate the local growth in spatial discretization error and to link it with temporal error given in Eq. 4 [7]:

$$\|le(t_{n+1})\| = \varepsilon \|E_s(t_{n+1})\| \tag{4}$$

where ε is the adjusting parameter. In the subsequent section, a brief discussion of the estimation of local growth in spatial discretization error and novelty regarding the different parameter optimization is presented. Since Eq. (2) has been representing the reacting flow, the ordinary differential equation function given in Eq. (3) will be of the form:

$$F_N(t, V(t_n)) = F_N^f(t, V(t_n)) + F_N^s(t, V(t_n)) \tag{5}$$

where $F_N^f(t, V(t_n))$ and $F_N^s(t, V(t_n))$ stands for convective term discretization and source term integration arising from atmospheric chemistry. Applying second order upwind scheme and midpoint method for source term integration will give the convective flux at j^{th} grid point of the form:

$$F_j^f(t_n, V_j(t_n)) = \frac{\Delta x}{\Delta t} \left[1 + \frac{1}{2}(B(r_j, 1) - \frac{1}{r_j-1} B(r_j - 1)) \right] (V_j(t_n) - V_{j-1}(t_n)) \tag{6}$$

and integration of the source term with the midpoint gives

$$F_j^s(t_n, V(t_n)) = \psi(V_j(t_n)) \tag{7}$$

which leads the Eq. (6) to the following form for j^{th} grid point

$$F_j^f(t_n, V_j(t_n)) = \frac{\Delta x}{\Delta t} \left[1 + \frac{1}{2}(B(r_j, 1) - \frac{1}{r_j-1} B(r_j - 1)) \right] (V_j(t_n) - V_{j-1}(t_n)) - \psi(V_j(t_n)) \tag{8}$$

and for parameter clarification [3]. Applying different discretization and integration to Eq. (2), according to requirement of the LEPLUS error control strategy, we have

$$\dot{v}_{n+1}(t_n) = G_N(t_n, v_{n+1}(t_n)) \tag{9}$$

having initial condition $v_{n+1}(t_n) = V(t_n)$ and $V(t_n)$ is the solution of Eq. (2) at the n^{th} time step. Finally, the local growth in time spatial discretization error will be the difference between primary solution and secondary solution of Eq. (3) and Eq. (9) given as

$$E_s(t_{n+1}) = V(t_{n+1}) - v_{n+1}(t_{n+1}) \tag{10}$$

and it will attain the following form after applying NDF2 method as a time integrator to Eqs. (2) and (9) given as

$$E_s(t_{n+1}) = \Delta t (\alpha_q \gamma_q + \frac{1}{q+1}) [F_N(t_{n+1}, V(t_{n+1})) - G_N(t_{n+1}, V(t_{n+1}))] \tag{11}$$

and for constants α_q and γ_q [1] and q is the order of method. The Eq. (11) can be further modified by writing it in terms of residual of auxiliary ODE given by Eq. (9):

$$E_s(t_{n+1}) = \Delta t (\alpha_q \gamma_q + \frac{1}{q+1}) [r(t_{n+1}, V(t_{n+1}))] \quad (12)$$

which is the local growth in spatial discretization error and $r(t_{n+1}, V(t_{n+1}))$ is the residual of auxiliary ODE defined by Eq. (9). So, the time tolerance for 'TOL(tn+1)' for the LEPUS control strategy being implemented at the step t_{n+1} is given by

$$TOL(t_{n+1}) = \left\| \alpha_q \gamma_q + \frac{1}{q+1} [r(t_{n+1}, V(t_{n+1}))] \right\| \quad (13)$$

The Eq. (12) predicts that error tolerance is proportional to the local error, and indirectly to the global error which is not true in connection with the LEPS control strategy [5, 7]. Additionally, the procedure of acceptance of the time step size is related to the following criteria.

$$\left\| \frac{le(t_{n+1})}{\varepsilon E_s(t_{n+1})} \right\| < 1 \quad (14)$$

The cognition of Eq. (14) shows that the adjusting parameter ε has a close link with accepting and rejecting the time step and was kept constant in previous studies [3, 5, 7]. The decision criteria defined by Eq. (14) will give unnecessary acceptance and rejection of time step that will affect the performance of the code. The reason is the unpredictable behavior of local growth in spatial discretization error $E_s(t_{n+1})$ due to the model stiffness and which is being handled with the inclusion of the variable adjusting parameter ε .

Consequently, the adjusting parameter is linked with species gradient present in the chemical model and is varied adaptively. Therefore, the modified arc-length adaptive mechanism in time is used that links the time derivative to the ratio of two consecutive time steps in the following way [9].

$$\frac{\Delta t_{n+1}}{\Delta t_n} = \left\| \sqrt{\frac{(\Delta t)^2 + (\dot{V}(t_n) - \dot{V}(t_{n-1}))^2}{\Delta t}} \right\| \quad (15)$$

where $\dot{V}(t_n)$ and $\dot{V}(t_{n-1})$ is the time derivative at two consecutive time steps, defined by Eq. (3). Naturally, at time step Δt_{n-1} the Eq. (15) is satisfied with adjusting parameter ε_0 and we are interested that at time step Δt_n the relation $\left\| \frac{le(t_n)}{\varepsilon \Delta t_n TOL} \right\| < 1$, must be satisfied for TOL given by the Eq. (14).

For small Δt ,

$$\left\| \frac{le(t_{n+1})}{\varepsilon_0 \Delta t_{n+1} TOL} \right\| \cong \left\| \frac{le(t_n)}{\varepsilon \Delta t_n TOL} \right\| \quad (16)$$

and combining it with Eq. (15) gives

$$\varepsilon = \varepsilon_0 \sqrt{1 + \frac{(\dot{V}(t_n) - \dot{V}(t_{n-1}))^2}{\Delta t^2}} \quad (17)$$

Because of the small-time step, the local and spatial discretization errors remain unchanged. Hence, Eq. (17) links the adjusting parameter with species gradient and it reduces to the original ε_0 [5, 7, 8] for species gradient remains constant. Hence, the combination of Eq. (14) and Eq. (17) has helped reduce the unnecessary acceptance and rejection of the number of steps. Therefore, the case of small-time tolerance given by Eq. (13) is adjusted using Eq. (17) as it includes the previous time gradient.

The other case when $E_s(t_{n+1})$ is higher than Eq. (14) will give unnecessary acceptance of step size and therefore Eq. (17) is modified in the following manner:

$$\varepsilon = \frac{\varepsilon_0}{\sqrt{1 + \frac{(\dot{V}(t_n) - \dot{V}(t_{n-1}))^2}{\Delta t^2}}} \quad (18)$$

The adaptive variation of adjusting a parameter ε based upon Eq. (17) and Eq. (18) along with Eq. (14) has improved performance of ILEPUS compared to the original LEPUS approach [5, 7, 8]. It is novelty in the existing theory of the LEPUS control strategy based on local growth in spatial discretion error given by Eq. (4). Recalling the NDF2 method, as discussed in [1] has been used as a time integrator. Its attractive feature includes the usage of 1.26 times higher step size compared to the BDF2 method and is written in the following form:

$$\frac{V(t_{n+1}) - \sum_{i=1}^4 V(t_{n+1-i}) \alpha_i}{\Delta t \tilde{\gamma}} - \alpha_q \frac{V(t_{n+1}) - V^p(t_{n+1})}{\Delta t \tilde{\gamma}} - F(t_{n+1}, V(t_{n+1})) = 0 \quad (19)$$

where the typical values of various parameters are $\alpha_1 = 4/3$, $\alpha_2 = 1/3$, $\tilde{\gamma} = 2/3$ and $\alpha_q = -1/9$ respectively. The above equation can be further simplified in the following form.

$$V(t_{n+1}) + (\alpha_q V^p(t_{n+1}) - \sum_{i=1}^4 V(t_{n+1-i}) \alpha_i) - \Delta t \tilde{\gamma} F(t_{n+1}, V(t_{n+1})) = 0 \quad (20)$$

where $\alpha_q = -1/9$ and it implies that $\tilde{\gamma} = 0.9 \tilde{\gamma}$. Using the modified Newton modified method the above equation will take the following form for (m+1)th correction iteration:

$$[1 - \Delta t \tilde{\gamma} J] \Delta V_m = r(t_{n+1}^m) \quad (21)$$

Where,

$$\begin{cases} J = \frac{\partial F}{\partial V} \\ r(t_{n+1}^m) = -V^m(t_{n+1}) + Z_n + \Delta t \tilde{\gamma} F(t_{n+1}, V_{n+1}^m) \\ \Delta V_m = (V(t_{n+1}^{m+1}) - V(t_{n+1}^m)) \\ Z_n = \sum_{i=1}^q V_{n+1-i} \alpha_i - \alpha_q V_{n+1}^p \end{cases} \quad (22)$$

Consequently, the Jacobian matrix given by Eq. (21) will take the following form according to ODE function defined by Eq. (3)

$$[1 - \Delta t \tilde{\gamma} J] = [1 - \Delta t \tilde{\gamma} J^f][1 - \Delta t \tilde{\gamma} J^s] + (\Delta t)^2 \quad (23)$$

The first term on the right side of Eq. (23) originates from the Jacobian of flow part and the second term shows the Jacobian of chemistry term discussed in Eq. (1). Since the source term is dominant in the atmospheric dispersion arising from chemical mechanism, the Eq. (23) reduces to the following form:

$$[1 - \Delta t \dot{\gamma} J] = [1 - \Delta t \dot{\gamma} J^s + (\Delta t \dot{\gamma})^2 J^s J^f] \quad (24)$$

The simplification procedure relating to Jacobian evaluation is different, as discussed in [6] and has been successfully applied here.

Case 1: Simulation of compressible flow with equilibrium chemistry in one-dimensional shock tube was done with the initial molar ratio, 2/1/7 of species H₂/O₂/Ar with the assumption that these are thermally perfect gases. The reaction mechanism is related to burning of hydrogen and oxygen [4]. Initially, the temperature and pressure on the left side of the shock tube were 400 k and 8000 m⁻³ respectively, while on the right side, these parameters were 1200 k and 80000 m⁻³, respectively. The procedure for calculating the density and extension of equation state of multi-species is given in [4]. The total energy E of the mixture is calculated according to the procedure:

$$E = -p + \frac{\rho u^2}{2} + \rho h \quad (25)$$

and the procedure for enthalpy for thermally perfect system was also elaborated in ref. [4]. The Fig. 1 shows the results are comparable to the earlier predicted results [4], however with rapid convergence. For further information the results for LEPS can be seen in [7].

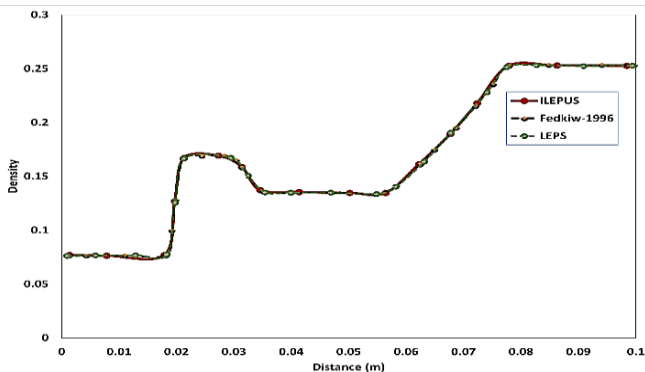


Fig. 1: Simulation results of the density in compressible flow having equilibrium chemistry.

Case II: A simple model to represent the troposphere reaction mechanism has been simulated [13]. In this case, there are only seven species, and the stiffness naturally prevails due to the competition of volatile organic compounds (VOCs), which occur much less time than the fast-equilibrating inorganic reactions (3) and (4). Being a highly lumped species ROC in volatile reactions does not justify the actual emission generated in the environment, but here the main purpose is to investigate the adaptive error control strategy in terms of its efficiency and accuracy of the predicted results. The simulation time is two days with the assumption of background-free atmosphere. The span of the domain is 5 km and the transmissive boundary conditions have

been assumed on the right-hand side, while on the left source has been assumed with the concentration: NO=35 μg/cm³ NO₂=40 μg/cm³, which were similar to experimental data acquired in Changchun city of China [10].

Generally, the atmospheric modeling reaction mechanism blends both; photolysis and temperature dependent reactions. The photolysis rate constant, which has a direct relation with solar zenith angle, is given by the following relation:

$$k_p = ae^{(-b \sec(\phi))} \quad (26)$$

where a, and b are specific for each photolysis chemical reaction, φ is the solar zenith angle, which is estimated from the following expression:

$$\cos(\phi) = \cos(LHA) \cos(DEC) \cos(LAT) + \sin(DEC) \sin(LAT) \quad (27)$$

where the solar declination angle (DEC) is taken as 23.27 and the Latitude (LAT) is 43.92o. The remaining parameter local hour angle is given by:

$$LHA = \pi \left(1.0 + \frac{t}{4.32} + 4 \right)^0 \quad (28)$$

where 't' is time in seconds. Similarly, the temperature-dependent rate constants have been evaluated using Arrhenius expression given as:

$$k = AT \beta e^{\left(\frac{-E_a}{R_u T} \right)} \quad (28)$$

where parameters Ea, Ru and T stand for an experimental activation energy, the universal gas constant and temperature. The temperature T is a function of daytime and is given by the following expression:

$$T = 289.86 + 8.3 \sin(7.27 \times 10^{-5} t) - 1.96 \quad (29)$$

The initial conditions of different species for reaction mechanism are shown in table (1). This is one of the simplest models which completely describe the major nitrogen oxides behavior comprising of the VOCs compound as well. There are two routes related to production of NO₂. First route is combination of RP with NO and others is the results of combination of NO and O₃. Also, in the presence of sunlight the NO₂ reduces to NO and ozone (O₃) and this cycle is continued. The initial concentration used in the simulation is given in table (1).

Table 1: Initial concentration of species used for simulation

No.	Name of Species	μg/cm ³
1	NO ₂	1.5
2	NO	1.2
3	O ₃	1.4
4	ROC	1.5
5	RP	0.00
6	SGN	0.00
7	SNGN	0.00

Where the abbreviations used in table 1 are; ROC is the reactive organic compound, RP represents the radical pool, SGN

and SNGN show the stable gaseous and non-gaseous nitrogen compounds respectively. Similar mechanism has also been discussed by Zhong [14] in which the Reactive Organic Compound (ROC) and other compound listed in table (1) are ignored as its detail are given in Carpenter et al. [15]. At origin we have solved the rate equations for which the Eq. (1) reduces to following form:

$$\frac{dC}{dt} = P - LC \quad (30)$$

where c is species concentration, P and L are the production and loss term of the species and has the following forms for NO and NO₂

$$\frac{dNO}{dt} = r_3 - r_2 - r_4 \quad (31)$$

$$\frac{dNO_2}{dt} = r_2 + r_4 - r_3 - r_6 - r_7 \quad (32)$$

with initial condition NO=35 $\mu\text{g}/\text{cm}^3$ NO₂=40 $\mu\text{g}/\text{cm}^3$ and other species have same concentration as discussed in table (1). Where, r_i 's are the reaction rates of species [13]. Figures 2(a) and 2(b) represent the results of the above mentioned simple mechanism and experimental data for different sites in Changchun City [10]. Additionally, we have used the detail

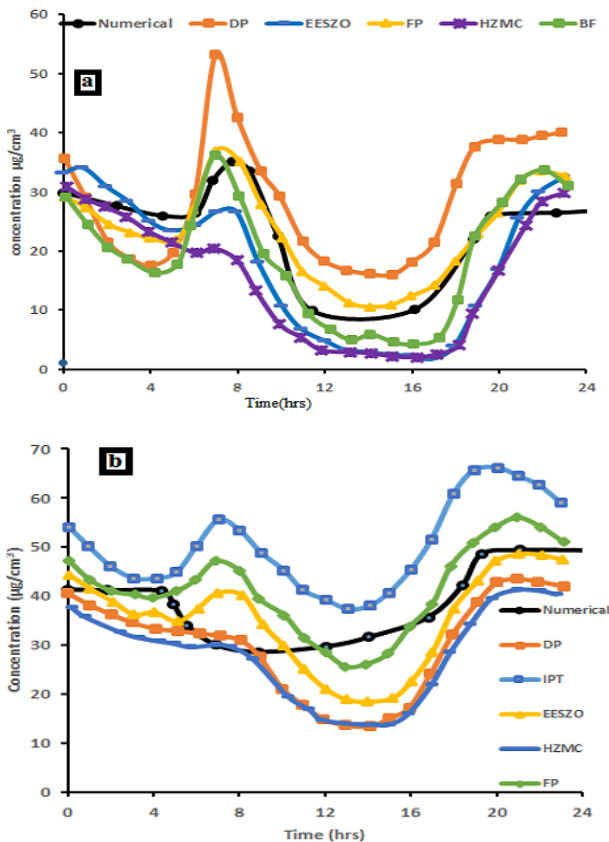


Fig. 2: (a) Shows the comparison of the simulated results of NO to that experimental data at different sites of Changchun city and (b) exhibits the comparison of NO₂.

model and no chemical reduction technique is applied as RP has been removed in ref. [16]. For comparison with experimental we have calculated the correlation coefficient defined in [12] and are presented table (2) for different sites in Changchun City [10]. For the accuracy comparison we have presented correlation coefficient between the simulated results and experimental data in table (2). These coefficients show the similarity of simulation results and the experimental data.

Table 2: Correlation coefficient between simulated results and experimental results, Neupane et al. [12]

Serial No	Sites	Correlation Coefficient for NO and NO ₂ at different sites	
		NO	NO ₂
1	DP	0.65146	0.81205
2	EES20	0.62384	0.738472
3	FP	0.75715	0.753293
4	HZMC	0.61705	0.798037
5	BF	0.61605	0.693662
6	IPT	0.75385	0.717315

The one-dimensional dispersion calculation results are presented in Fig. 3 (a) and Fig. 3 (b) for NO and NO₂ respectively using the ILEPUS and the LEPS respectively. Since there was no experimental data for one dimensional case, therefore, to justify its accuracy, we have solved one known problem given in case (I) for which results have already been shown in Fig. (1).

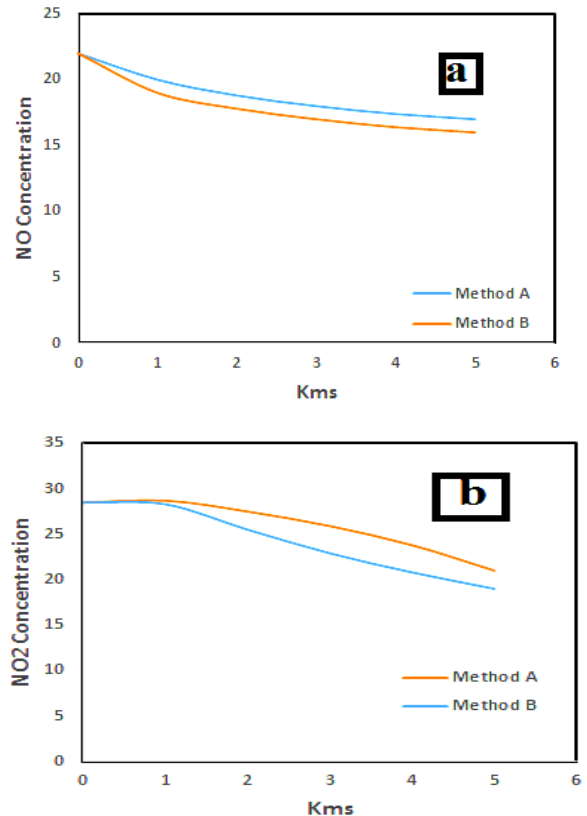


Fig. 3: Dispersion of the one-dimensional NO and NO₂ for five kilometers using constant wind velocity for approximately 10 hours.

3. Results and discussion

Novel error balance approach ILEPUS was observed to produce comparable results with LEPS and methodology of reference [4] for the compressible flow problem in one-dimensional shock tube with equilibrium chemistry. Similarly, for one-dimensional dispersion problem with seven reactions and reactive species, ILEPUS results were found to be compatible with the LEPS (see Fig. 3 (a) and Fig. 3 (b)). Additionally, no reduction techniques were used to further simplify the reaction mechanism as suggested in reference [16]. Comparing the experimental data, it was observed that the diurnal trends in NO and NO₂ concentrations were similar everywhere. Moreover, the peak can be seen around 9 AM [4]. The similarity in trends (see Fig. 2) was checked by means of the correlation coefficient. The lowest correlation coefficients values for NO and NO₂ were 0.61605 and 0.693662, respectively. Since the concentrations exhibit variations due to local atmospheric conditions, it is difficult to

obtain numerically close values. It should be noted that for both one and two-dimensional reaction-dispersion problems, the ILEPUS took a lesser number of steps than that of the LEPS to approach the same level of accuracy.

For simplicity, the diffusion term has been ignored. It was observed that ILEPUS has predicted results to the comparable accuracy as that of LEPS for the reference problem [16] with lesser number of steps. ILEPUS and LEPS results for various computational parameters are summarized in table 4.

It can be concluded that the results with ILEPUS are accurate that of LEPS even for RTOL=0.01, with less number of steps and other computational parameters. This conclusion further reinforces the assumption that the ILEPUS is more efficient even in solving the complex case of high Lipschitz constant. The adjusting parameter ϵ_0 in table (5) was varied adaptively using Eqs. (17) and (18) after using reference initial value [1, 3, 5, 6].

Table 4: Results of one-dimensional atmospheric problem with uniform grid using the ILEPUS and the LEPS

Domain Type	Grid Points	Methods	ATOL or ϵ_0	RTOL	Nsteps	Fun	Jac
One dimensional case	321	LEPS	105	0.01	5193	6962	4030
				0.001	5421	7188	4247
		ILEPUS	0.3		5011	6362	3066

4. Conclusion

It can be concluded that the innovative error balance approach ILEPUS was developed to numerically solve the coupled reaction-dispersion problems in the atmosphere. It establishes the direct relationship between the global error and tolerance based on local growth in spatial discretization error. The abrupt change in the error tolerance due to stiffness is linked with the adaptive variation of the adjusting parameter, which is the novelty in the existing theory of error balance approach. Further tuning is performed using the Jacobian evaluation by linking with local growth in spatial discretization error. The method was applied to solve three problems of varying complexity: (1) compressible flow with equilibrium chemistry in one-dimensional shock tube (2) one-dimensional reaction-dispersion with seven species, and (3) Two-dimensional reaction-dispersion with twenty species. In all cases, the results were numerically consistent with the conventional LEPS methodology but with fewer computational steps. In addition, predictions of NO and NO₂ concentrations were positively correlated with observed data in Changchun city of China supporting the hypothesis of modeling adequacy with seven reacting species. For the third problem, the computing efficiency of ILEPUS was also found to be superior to that of LEPS. The efficiency of ILEPUS would bring more complicated problems such as more species, actual weather conditions etc. amenable to computations.

References

- [1] I. Ahmad and M. Berzins, "An algorithm for ODEs from atmospheric dispersion problems", *Appl. Numer. Math.*, vol. 25, no. 2-3, pp. 137-149, 1997.
- [2] L.K. Peters et al., "The current state and future direction of Eulerian models in simulating the tropospheric chemistry and transport of trace species: a review", *Atmos. Environ.*, vol. 29, no. 2, pp. 189-222, 1995.
- [3] M. Berzins, A.S. Tomlin, S. Ghorai, I. Ahmad, and J. Ware, "Unstructured Adaptive Mesh MOL Solvers for Atmospheric Reacting-Flow Problems", in *Adaptive Method of Lines*, Chapman and Hall/CRC, pp. 337-372, 2001.
- [4] R.P. Fedkiw, "A survey of chemically reacting, compressible flows", University of California, Los Angeles, 1996.
- [5] J. Lawson, M. Berzins and P.M. Dew, "Balancing space and time errors in the method of lines for parabolic equations", *SIAM J. Sci. Stat. Comput.*, vol. 12, no. 3, pp. 573-594, 1991.
- [6] M. Berzins and J.M. Ware, "Positive cell-centered finite volume discretization methods for hyperbolic equations on irregular meshes," *Appl. Numer. Math.*, vol. 16, no. 4, pp. 417-438, 1995.
- [7] I. Ahmad and M. Berzins, "MOL solvers for hyperbolic PDEs with source terms," *Math. Comput. Simul.*, vol. 56, no. 2, pp. 115-125, 2001.
- [8] M. Berzins, "Temporal error control for convection-dominated equations in two space dimensions," *SIAM J. Sci. Comput.*, vol. 16, no. 3, pp. 558-580, 1995.
- [9] Q. Sheng and A.Q. M. Khaliq, "Linearly implicit adaptive schemes for singular reaction-diffusion equations," in *Adaptive Method of Lines*, Chapman and Hall/CRC, 2001, pp. 283-314.
- [10] L. Wang, J. Wang, X. Tan, and C. Fang, "Analysis of NO_x pollution characteristics in the atmospheric environment in Changchun City," *Atmosphere (Basel)*, vol. 11, no. 1, p. 30, 2020.
- [11] K. Gasmi, A. Aljalal, W. Al-Basheer, and M. Abdulahi, "Analysis of NO_x, NO and NO₂ ambient levels in Dhahran, Saudi Arabia," *Urban Clim.*, vol. 21, pp. 232-242, 2017.

- [12] A. Neupane, N. Raj, R. Deo, and M. Ali, "Development of data-driven models for wind speed forecasting in Australia," in *Predictive Modelling for Energy Management and Power Systems Engineering*, Elsevier, pp. 143–190, 2021.
- [13] M. Azzi, G.M. Johnson, and M.E. Cope, "An introduction to the generic reaction set photochemical smog mechanism", 1992.
- [14] J. Zhong, "Modelling air pollution within a street canyon", University of Birmingham, 2016.
- [15] L.J. Carpenter, K.C. Clemishaw, R.A. Burgess, S.A. Penkett, J.N. Cape, and G.G. McFadyen, "Investigation and evaluation of the NO_x/O₃ photochemical steady state", *Atmos. Environ.*, vol. 32, no. 19, pp. 3353–3365, 1998.
- [16] J.M. Haussaire and M. Bocquet, "A low-order coupled chemistry meteorology model for testing online and offline data assimilation schemes: L95-GRS (v1. 0)", *Geosci. Model Dev.*, vol. 9, no. 1, pp. 393–412, 2016.
- [17] T.J. Wallington, E.W. Kaiser, and J.T. Farrell, "Automotive fuels and internal combustion engines: a chemical perspective", *Chem. Soc. Rev.*, vol. 35, no. 4, pp. 335–347, 2006.
- [18] Y. Wu, F. Ma, and V. Yang, "Space-Time Method for Detonation Problems with Finite-rate Chemical Kinetics", *Int. J. Comput. Fluid Dyn.*, vol. 18, no. 3, pp. 277–287, 2004.

Nomenclature

a	Advection speed	Nsteps, Fun, Jac	Number of steps, function evaluation and Jacobian calculation during the solution
A, B	Local Error per step, per unit step	p	Pressure of the mixture
ATOL, RTOL	Absolute and Relative Tolerance	q	Order of the time integrator
C_i	Species Concentration of ith species	R_i	Reaction Mechanism for ith species
E	Total Energy of the mixture	t	time
E_i	Emission source of ith species	\mathbf{u}	General variable of partial differential equation
$E_s(t_{n+1})$	Local growth in time spatial discretization error	u_L, u_R	Left and right value of the general variables
E_a, R_u and T	experimental activation energy, the universal gas constants and temperature	$V(t_n)$	The numerical approximation of the true solution at time t_n
$F_N(t, V(t_n))$	Function of primary ordinary differential equation resulting from discretization of advection term and the integration of the source term	$\dot{v}_{n+1}(t_n)$	Second numerical approximation of the partial differential equation
$F_N^f(t, V(t_n))$	Discretization of the advection term with second order upwind scheme	X, Y	Space variables along x-axis and y-axis
$F_N^S(t, V(t_n))$	Integration of the source term	α_q	Co-efficient of the time integrator, NDF2 method
$G_N(t_n, v_{n+1}(t_n))$	Function of auxiliary ordinary differential equation resulting from discretization of advection term and the integration of the source term	$\tilde{\gamma}$	Coefficient of the function of the BDF method
h	Enthalpy	$\dot{\gamma}$	Coefficient of the function of the NDF2 method
J	Jacobian Matrix	Δx	Spatial discretization
J^f, J^s	Jacobian of the flow part and the source term	Δt	Time step
$k_{1,i}, k_{2,i}$	Wet and dry coefficient	\mathcal{E}	Balancing parameter which has been varied adaptively
kp	Photolysis rate constant	μ	Prefix of the general partial differential equation
K_x, K_y	Diffusivity coefficient in x-axis and y-axis	ρ	Density
LHA	Local Hour angles	$\psi(\mathbf{u})$	Source term
N	Number of Species	ϕ	Solar zenith angle